



Restratification by Mixed Layer Instabilities

Baylor Fox-Kemper and Raffaele Ferrari
MIT Earth, Atmospheric and Planetary Sciences Dept. and NOAA Climate and Global Change Program
MIT 54-1410, 77 Mass. Ave., Cambridge, MA 02139, baylor@alum.mit.edu

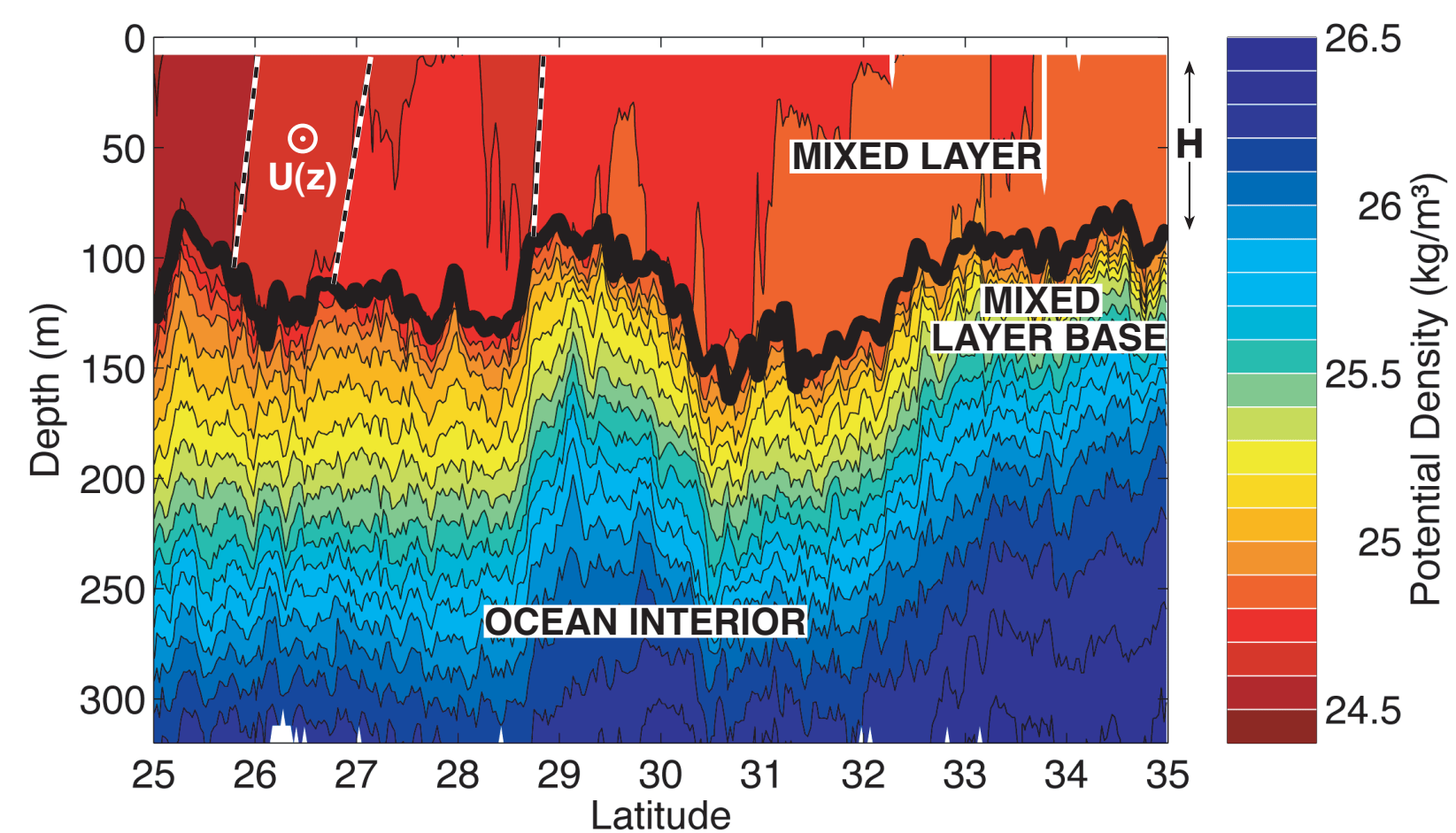
AMS 15th Conference on Atmospheric and Oceanic Fluid Dynamics



I. Abstract

We study the restratification of the oceanic surface mixed layer that results from lateral inhomogeneities in the surface density field. Mixed layer models are quite successful at reproducing the deepening of the mixed layer, but the restratification phase is not as well understood and model bias is especially large when there are horizontal variations in the density field. These lateral inhomogeneities give way to ageostrophic baroclinic instabilities which slump the horizontal density gradients under the effect of rotation. These mixed-layer instabilities (MLI) differ from ocean interior instabilities because of the weak surface stratification, and the fact that their lower 'boundary' is a density jump in the transition layer between the mixed layer and the ocean interior. Spatial scales are $O(1-10)$ km and growth rates are faster than a day. We use both linear stability analysis and fully nonlinear simulations to study the impact of MLI on mixed layer restratification. Finally we discuss the issue of parameterization of MLI-driven restratification in mixed layer models.

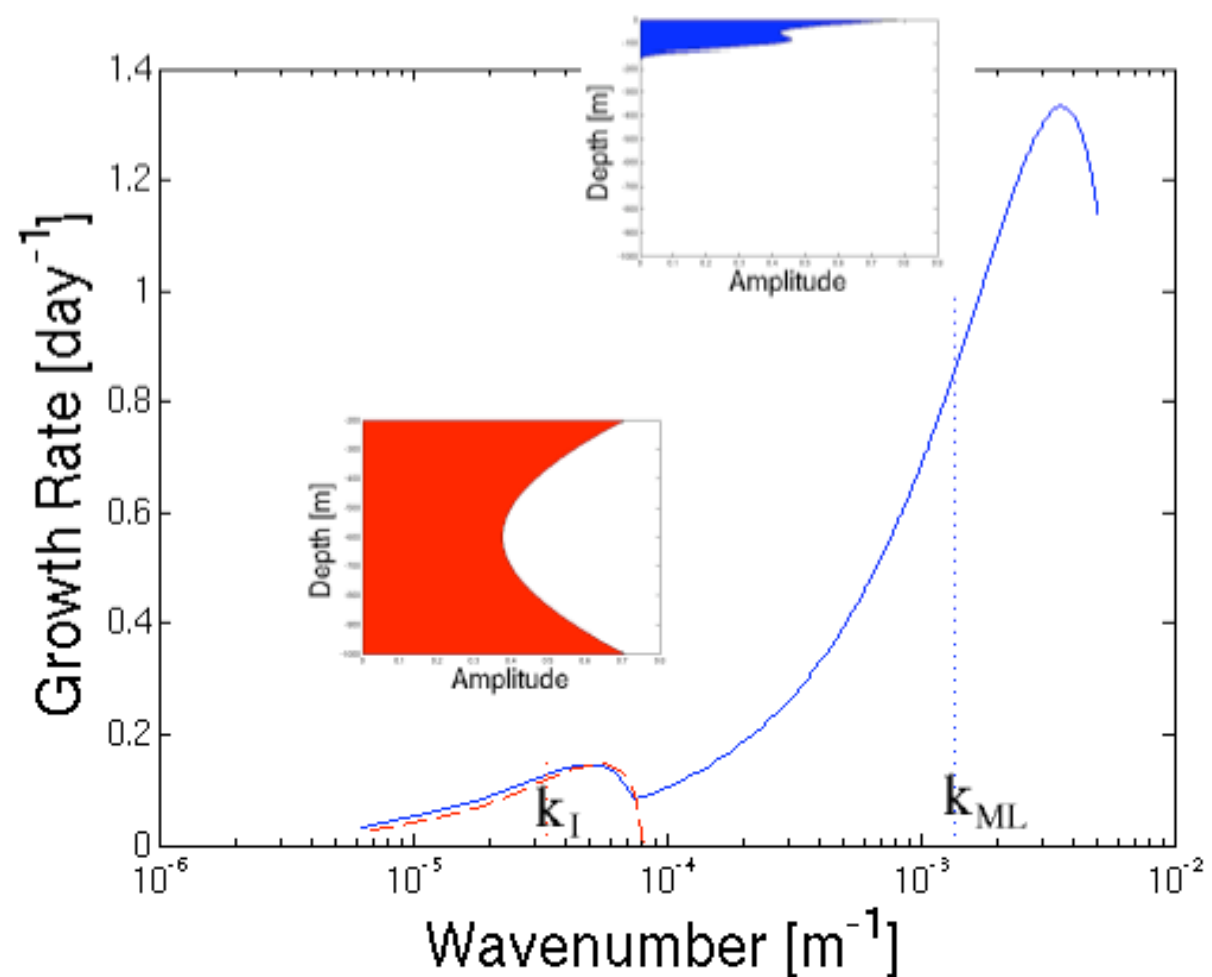
II. Ocean Mixed Layer



Potential density section from towing a CTD following a saw-tooth pattern in the Subtropical Gyre of the North Pacific between 25N and 35N at 140W. (Ferrari and Rudnick, 2000).

The ocean mixed layer (ML) is a layer of weak stratification in the upper 100 m overlying the more stratified thermocline. The ML is not horizontally homogeneous; there are numerous lateral density gradients. ADCP measurements collected during the same campaign confirm that the lateral density gradients are in geostrophic balance with a sheared velocity U_z as schematized here.

III. Restratification of the Ocean Water Column

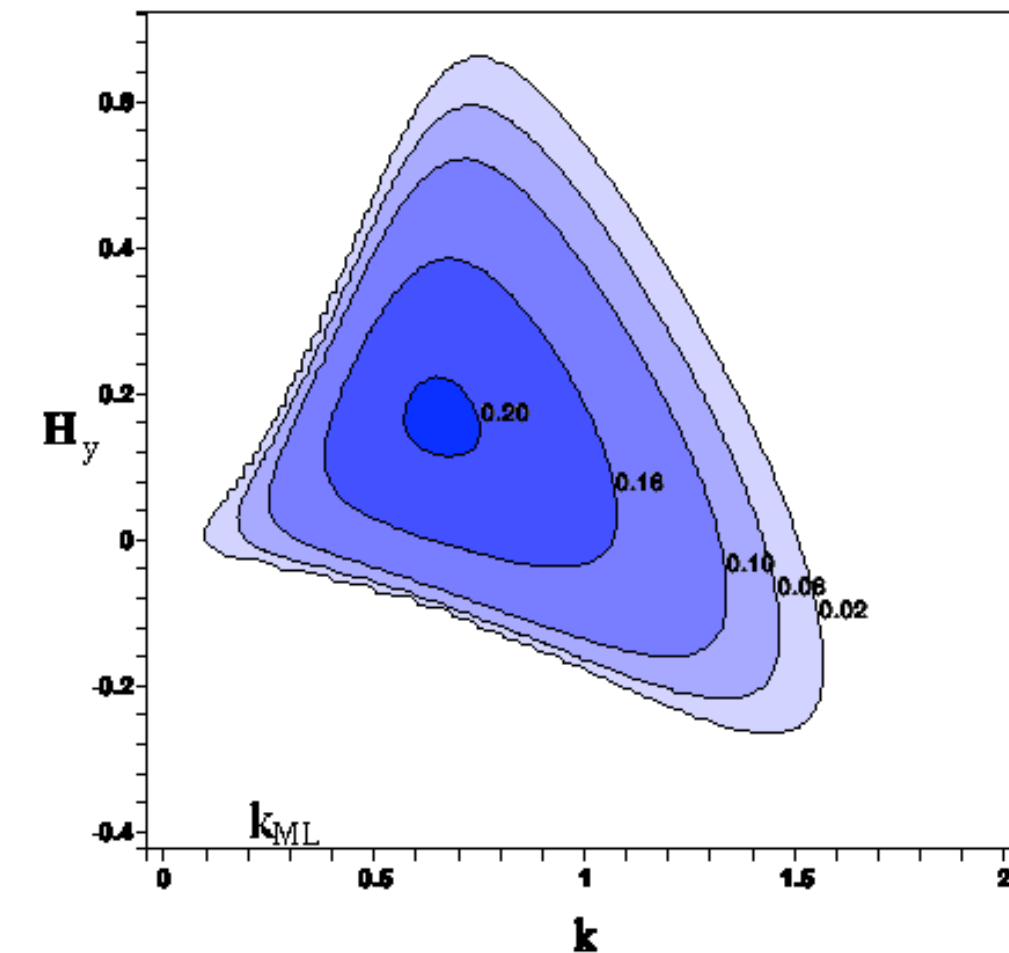


The linear instability of the upper 1000m of the ocean water column. The basic state is composed of a 200m deep ML with $N \approx 4 \times 10^{-4} s^{-1}$, $U_z = 2 \times 10^{-4} s^{-1}$, and $Ri = 3.6$ sitting on a 800m thermocline with $N \approx 4 \times 10^{-3} s^{-1}$, $U_z = 2 \times 10^{-4} s^{-1}$ and $Ri = 360$. For comparison, shown in red is the instability of the 800m ocean interior alone with a rigid lid replacing the ML. Also shown are the amplitude versus z of the fastest growing interior mixed layer modes, and the inverse deformation radii.

Consider the stability of the upper ocean water column. Its instability is dominated by two distinct modes: an interior instability with wavelength close to $2\pi/3$ times the internal deformation radius (≈ 60 km) shown in red and a mixed-layer instability (MLI) peaking at wavelength close to $2\pi/3$ times the ML deformation radius (≈ 1.5 km) shown in blue. The interior instability has a spatial structure (inset red) spanning the whole thermocline depth and represents the mesoscale restratification due to quasi-geostrophic baroclinic instability (Eady, 1949). The MLI (inset blue) is confined to the ML and represents restratification due to ageostrophic instability of the upper 200 m (Stone, 1971).

MLI and interior modes roughly agree with the Eady (1949) model. They possess exponential edge waves trapped to the top and bottom of their domain. When these edge waves interact, a linear instability results. Both instabilities extract available potential energy stored in the horizontal density gradients, resulting in restratification.

Mixed layer instabilities (MLI) differ notably from those in the thermocline because of the weak stratification ($Ri=O(1)$, ageostrophy) and the presence of a moving interface at the base (a tilting base provides a topographic β -like effect). If we focus only on the MLI, a linearized ML dynamics that includes a moving density surface as a bottom boundary condition are given by the following equations and growth rate, where $\eta(t)$ is the ML base displacement and H_y is the ML base tilt. (see next column...)



The linear instability of $Ri=2$ (MLI-appropriate) primitive equations as a function of k (Rossby number units) and H_y (slope of ML isopycnal units). The maximum growth rate is approximately half a day. Equations below:

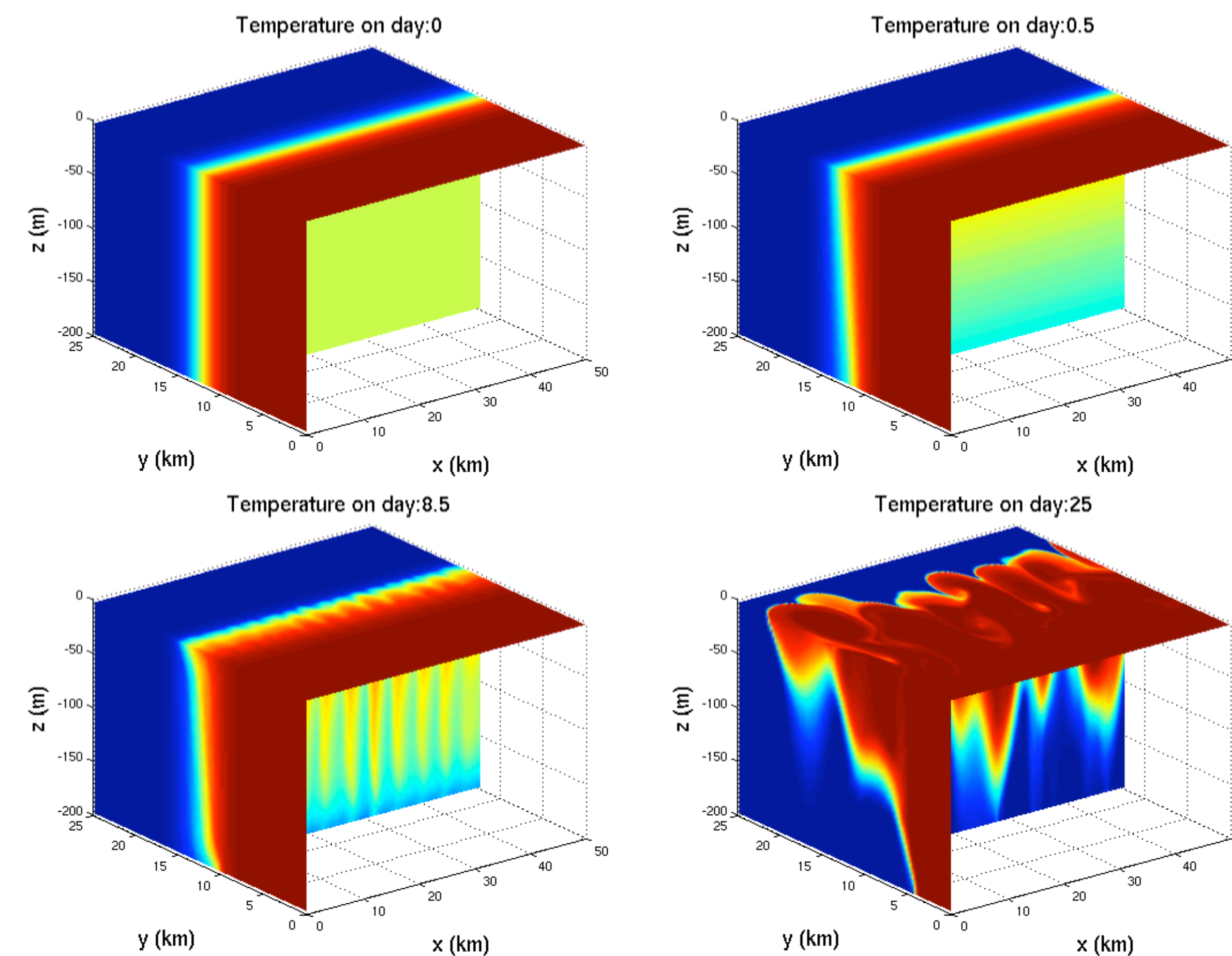
$$\begin{aligned} U(z) &= z & B(y, z) &= z + Ri^{-1}y, & H(y) &= 1 + H_y y, \\ (\partial_t + ikz)u + w - v + ikRip &= 0, \\ (\partial_t + ikz)v + u + iRip &= 0, \\ \delta^2(\partial_t + ikz)w + Rib + Ri\partial_z p &= 0, \\ (\partial_t + ikz)b + \frac{1}{Ri}v + w &= 0, \\ iku + ilv + \partial_z w &= 0, \\ z=0 \rightarrow \partial_t \eta + U_0 ik \eta + v H_y - w_0 &= -w_{en} = 0, \\ z=0 \rightarrow p_0 &= \Delta B \eta, \end{aligned}$$

For the ageostrophic problem, the fastest growing mode obeys $Ro^2 Ri = O(1)$. For MLI, $Ri=O(1)$, thus $Ro=O(1)$ and the instability is strongly ageostrophic.

Unlike $H_y = 0$, the ML tilt gives a low wavenumber cutoff. At high wavenumbers the instability is cured as in Eady (1949): the edge waves are too short to interact. Slab ML models do not possess exponentially-trapped edge waves and thus predict an ultraviolet catastrophe at high wavenumbers.

IV. Nonlinear Geostrophic Adjustment

Finite-amplitude, nonlinear aspects of MLI development allow the direct study of eddy mixing and restratification rates that may be utilized in parameterizations. We consider the geostrophic adjustment of initially-vertical density surfaces in a $200m \times 25km \times 50km$ channel (representing a section of the ML after the passage of a storm or isolated convective event):



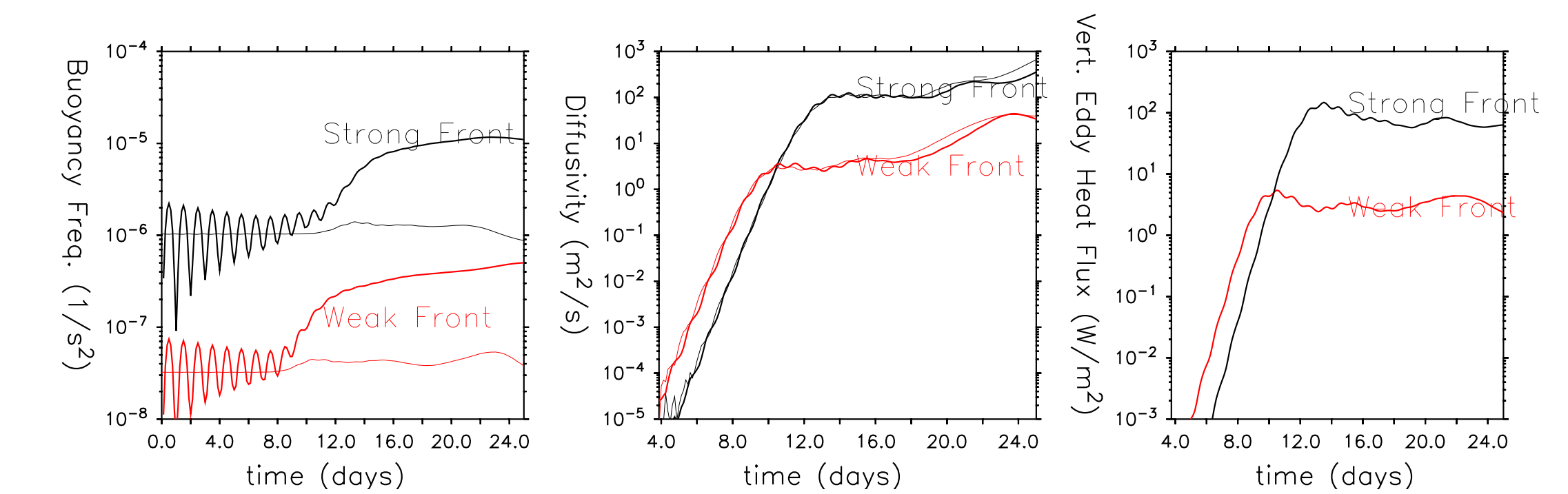
Snapshots of geostrophic adjustment and instability. Total density difference: 0.008 kg/m^3 .

Initially, the density surfaces drop gravitationally into an inertial oscillation about the state where $\rho_z f / \rho_y^2 \approx Ri \approx 1$. This stage of the adjustment is detailed by Tandon and Garrett (1994) and Ou (1984). The first two snapshots show the range of this oscillation in our simulation.

However, this oscillating state is not stable to MLI. Initially they grow as Eady (1949)-like waves much as predicted by the preceding analysis and with the ageostrophic growth rates due to Stone (1972). Day 8.5 above shows these waves nicely. The waves extract available potential energy from the mean stratification and drive a slumping/restratification of the initial front.

The restratification is enhanced as the waves reach finite amplitude and begin to nonlinearly interact strongly. The fully nonlinear waves are shown at day 25 above. Note that their length-scale has increased dramatically, as expected from an inverse energy cascade.

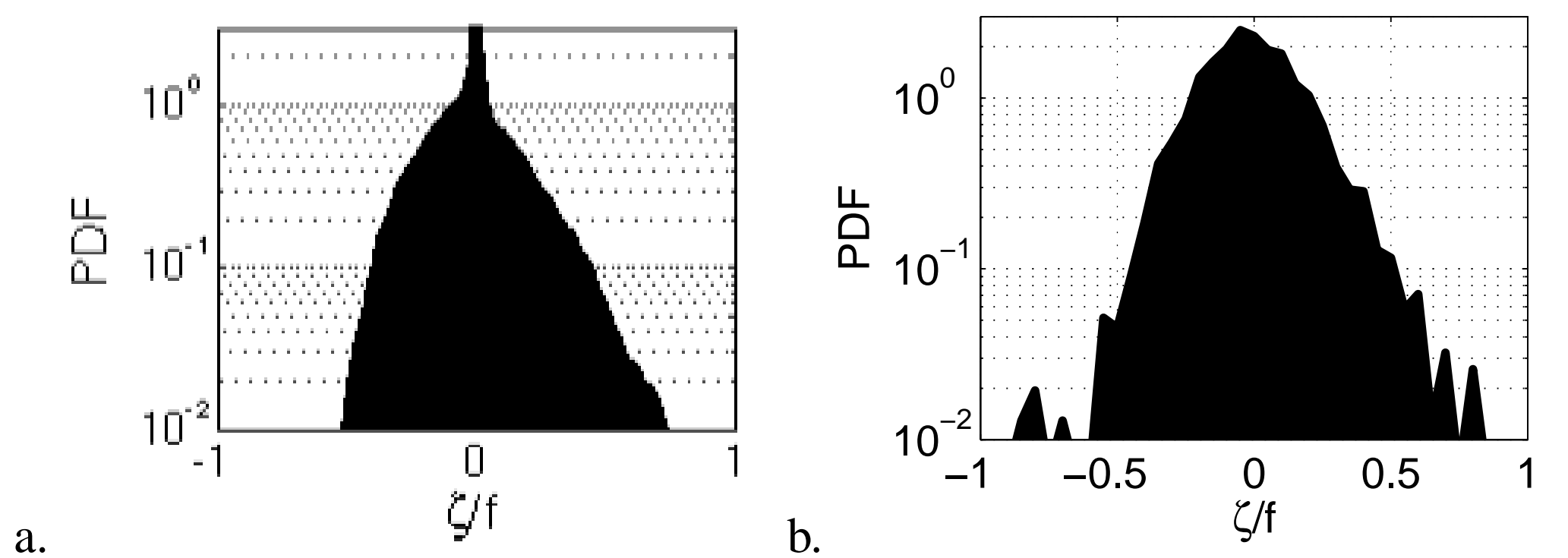
The following figure shows the restratification process for a weak front ($0.1K/10km$) and a strong front ($0.5K/10km$). Note the initial inertial oscillations and the significantly stronger restratification that occurs as the MLI develop. The effect of restratification by MLI may be parameterized by a Gent and McWilliams (1990) parameterization. However unlike in the ocean interior where a diffusivity of $O(1000 \text{ m}^2/s)$ is appropriate, we see that for MLI, $O(10-100 \text{ m}^2/s)$ is better. Previous attempts to use Gent and McWilliams (1990) too rapidly restratified the ML, but they used interior values of Gent-McWilliams diffusivity rather than MLI diffusivity values. Still, the implied magnitude of MLI's vertical eddy heat flux is significant compared to other mixed layer processes (e.g., diurnal-average surface fluxes and entrainment $O(100)W/m^2$).



Eddy statistics from two nonlinear calculations with different initial front strength.

VI. Spirals on the Sea?

Munk and Armi (2001) have recently noted the significance and ubiquity of $O(1-10 \text{ km})$ spirals of surfactant on the ocean surface. These spirals have a preferentially cyclonic rotation, and are often seen after long periods of hot weather. We note that the preferentially-cyclonic eddies formed by MLI in our nonlinear simulation share these features, and share the preference for cyclonic rotation to a realistic degree (see figure below). Ultimately, this can be attributed to the conservation of initially-vanishing potential vorticity.



Probability density function of relative vorticity divided by Coriolis parameter. (a) The numerical simulation at day 25, and (b) ADCP measurements in the North Pacific (Rudnick, 2001).

VI. Conclusions

- MLI are ubiquitous in mixed-layers possessing lateral variations in density.
- They are small in scale $O(1-10km)$ and fast-growing $O(\leq 1 \text{ day})$.
- They are ageostrophic and do not possess an ultraviolet catastrophe.
- They do a large share of the restratification.
- They are parameterizable via a Gent and McWilliams diffusivity $O(10 - 100 \text{ m}^2/s)$.
- Look for Boccaletti et al. (2005)!

References

Boccaletti, G., R. Ferrari, and B. Fox-Kemper: 2005, Mixed layer instabilities. In preparation.
Eady, E. T.: 1949, Long waves and cyclone waves. *Tellus*, **1**, 33-52.
Ferrari, R. and D. Rudnick: 2000, The thermohaline structure of the upper ocean. *Journal of Geophysical Research*, **105**, 16,857-16,883.
Gent, P. R. and J. C. McWilliams: 1990, Isopycnal mixing in ocean circulation models. *Journal of Physical Oceanography*, **20**, 150-155.
Munk, W. and L. Armi: 2001, Spirals on the sea: A manifestation of upper-ocean stirring. *Proceedings of the 12th 'Aha Huiho' a Hawaiian Winter Workshop*.
Ou, H.: 1984, Geostrophic adjustment: A mechanism for frontogenesis? *Journal of Physical Oceanography*, **14**.
Rudnick, D.: 2001, On the skewness of vorticity in the upper ocean. *Geophysical Research Letters*, **28**.
Stone, P. H.: 1971, Baroclinic stability under non-hydrostatic conditions. *Journal of Fluid Mechanics*, **45**.
— 1972, On non-geostrophic baroclinic stability. Part III. The momentum and heat transports. *Journal of the Atmospheric Sciences*, **29**.
Tandon, A. and C. Garrett: 1994, Mixed layer restratification due to a horizontal density gradient. *Journal of Physical Oceanography*, **24**.